Available online at www.sciencedirect.com

ScienceDirect

IFAC Papers Online CONFERENCE PAPER ARCHIVE

IFAC-PapersOnLine 48-23 (2015) 477–482

Set-based MPC with an Application to Enhanced Local Hyperthermia for Cancer Treatment

Xi Luo * **Bram de Jager** * **Edwin Heijman** **
W.P.M.H. (Maurice) Heemels *

* *Department of Mechanical Engineering, Eindhoven University of Technology, Eindhoven, The Netherlands (e-mail: {X.Luo, A.G.de.Jager, W.P.M.H.Heemels}@tue.nl)*
** *Philips Research Europe, Department Minimally Invasive Healthcare, Center for Imaging Research and Education (CIRE), Eindhoven, the Netherlands (e-mail: edwin.heijman@philips.com)*

Abstract: In this paper we propose a novel MPC scheme based on set theory that controls the temperature distribution in body tissue with the purpose of realizing local hyperthermia for improved cancer treatment. A new scheme is needed as there is no equilibrium nor invariant subset in the set of desirable temperature distributions subject to input and output constraints. The scheme fulfills the control objectives by using a dual-mode control strategy that steers the initial state to an appropriate reference set and keeps it inside the set of desirable temperature distributions for the (finite) length of the therapy duration. Feasibility of the scheme is guaranteed by off-line set-based computations. The online computations are formulated as standard quadratic programs. A numerical example is included to demonstrate the successful control of the transient temperature distribution in a one dimensional space.

1. INTRODUCTION

Local hyperthermia, as an adjuvant treatment, mildly heats body tissue within a certain specific region (locally) to the objective temperature ($T_{obj} = 41.5$[°C]) while keeping the temperature below the cell killing temperature ($T_{max} = 43$[°C]) during transients. This technique is of high practical interest in cancer and malignant tumor treatments as it results in enhanced radiotherapy or chemotherapy efficacy and reduced side effects, Overgaard (1989); Issels (2008). In combination with Temperature-Sensitive Liposomes (TSL), local hyperthermia can also be used to increase the anticancer drug's therapeutic window and the efficacy via temperature triggered drug release, Gaber et al. (1995).

One device used for applying non-invasive concentrated thermal dose in body tissue is the Philips High Intensity Focused Ultrasound (HIFU) transducer, which is a 256-element phased array transducer embedded in a patient table. It can be used to heat the body tissue by generating a high frequency (1.2 [MHz]) and focused acoustic field, Hynynen et al. (2004). By manipulating the phase difference among elements, the focal spot can be steered such that different parts of body tissue are heated individually. Non-invasive and tissue-independent temperature measurement can be achieved by using Magnetic Resonance (MR) thermometry based on water proton resonance frequency shift (water PRF), Rieke and Pauly (2008). The Philips clinical Magnetic Resonance guided High Intensity Focused Ultrasound (MR-HIFU) sonalleve system contains both these elements and can be applied to realize noninvasive and feedback-controlled local hyperthermia inside body tissue, Hijnen et al. (2012); de Smet et al. (2011).

Several approaches have been used for realizing a local hyperthermia in a treatment region larger than the focal spot size, Mougenot et al. (2009); Salomir et al. (2000), which use pre-defined sonication trajectories and a Proportional-Integral-Derivative (PID) power controller based on temperature feedback. Since the sonication trajectories are static while tissue's heat diffusion and perfusion effects are dynamic, temperature variance within a treatment region becomes large in space. As a consequence, these controllers significantly limit local hyperthermia's therapeutic efficacy and are, therefore, not preferred in clinical applications. In addition, these controllers are also considered inefficient due to conservative spiral sonication trajectory references.

Besides small temperature variance, safety is of great importance for local hyperthermia, in the sense that the maximum temperature in body tissue is restricted below T_{max}. With the ability to handle constraints explicitly, it is of interest to apply Model Predictive Control (MPC) for the realization of local hyperthermia. However, as the therapeutic efficacy is triggered by temperature elevation, a distinct temperature drop is expected at the boundary of a treatment region to guarantee minimal side effects for surrounding healthy tissue. Since it is not feasible to have a non-invasive heat sink inside body tissue, a steep temperature gradient descent cannot be maintained for (infinite) long time. Hence, there is no equilibrium nor a (non-empty) positively invariant subset in the set of desired temperature profiles (under the given constraints). This renders many existing MPC schemes unsuitable for the realization of local hyperthermia as they offer the asymptotic stabilization of an equilibrium or a positively invariant set, see e.g. the overviews Mayne et al. (2000); Maciejowski (2002); Camacho and Bordons (2007); Rawlings and Mayne (2013).

This paper contributes to local hyperthermia by introducing a novel dual-mode set-based MPC, which explicitly considers tissue's thermal dynamics, therapy requirements and safety constraints. Different from existing MPC schemes, the proposed dual-mode MPC scheme success-

2405-8963
Peer review under responsibility of International Federation of Automatic Control.
10.1016/j.ifacol.2015.11.324

fully steers and maintains a transient temperature profile within the desired set, which does not contain any equilibriums nor other (non-empty) controlled positively invariant subsets, for a sufficiently long duration.

The outline of this paper is as follows. In section 2, the system description as well as the control objectives and the constraints for the local hyperthermia problem are introduced. Section 3 introduces the new dual-mode MPC scheme, which is followed by a performance validation in Section 4. Conclusions are stated in Section 5.

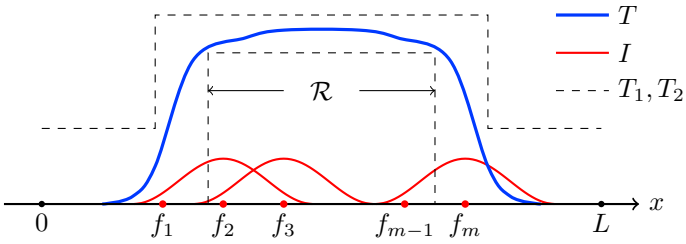

Fig. 1. One-dimensional example of the problem formulation with the considered region $\mathcal{Q} = [0, L]$, the treatment region $\mathcal{R}$, the focal spots f_i, $i = 1, \ldots, m$, the temperature increment profile T, the temperature bounds T_1, T_2 and the intensity profile I (plotted for focal spots f_2, f_3 and f_m individually).

2. PROBLEM DESCRIPTION

2.1 The Local Hyperthermia Setup

In clinical applications, the objective of local hyperthermia is to non-invasively create an elevated tissue temperature distribution in a particular region of a three-dimensional space. For ease of exposition and illustration, we study the one-dimensional case that contains all the necessary ingredients to be extended to higher dimensional setups in a straightforward manner. A schematic problem formulation is shown in Fig. 1. In a one-dimensional region $\mathcal{Q} \triangleq [0, L]$ with $L \in \mathbb{R}^+$ encompassing the surrounding tissue of the tumor, we consider a treatment region $\mathcal{R} \subset \mathcal{Q}$. Define the body temperature as $T_b = 37[^\circ\text{C}]$ and the temperature increment as $T(x,t)$ at location $x \in \mathcal{Q}$ and time $t \in \mathbb{R}_{\geqslant 0}$. According to the bio-heat equation Wissler (1998), the dynamic relationship between $T(x,t)$ and total power input profile $W(x,t)$ for $x \in \mathcal{Q}$ at time t is given by

$$\rho C \frac{\partial T(x,t)}{\partial t} = K \frac{\partial^2 T(x,t)}{\partial x^2} - W_b C_b T(x,t) + W(x,t), \tag{1a}$$

$$\text{s.t. } T(0,t) = T(L,t) = 0, \; T(x,0) = 0, \tag{1b}$$

where ρ is the material density, K is the heat diffusion coefficient, C and C_b are the tissue and the blood heat capacity and W_b is the blood mass flow rate in the tissue. The boundary and initial conditions are included in (1b). $\mathcal{Q}$ is assumed to be sufficiently large so that the temperature remains unchanged at $x = 0$ and $x = L$.

The HIFU transducer is used to (only) heat body tissue via a focused ultrasound acoustic field, which is given by a Gaussian thermal power intensity distribution $I : \mathcal{Q} \to \mathbb{R}_{\geqslant 0}$ (for a given and fixed focal point). The power input profile $W(x,t)$ can be controlled over time by changing the focus and the heating power. Due to hardware limitation, there are a finite number $m \in \mathbb{N}$ of focal spots $F = \{f_1, f_2, \ldots, f_m\}$ with $f_i \in \mathcal{Q}$, $i = 1, \ldots, m$, and the HIFU transducer can only focus at one position at a time. In order to have homogeneous thermal energy accumulation at different positions, switching among focal spots is necessary and possible. Although it takes a short time period to change the focal spot, the switching frequency is much higher than the time constants of the body tissue dynamics. The total power input $W(x,t)$ under fast switching is assumed equal to be the sum of the applied power $p_i(t)$ at each focal spot f_i, $i = 1, 2, \ldots, m$, i.e.,

$$W(x,t) = \sum_{i=1}^{m} p_i(t) I(x - f_i), \tag{2}$$

where we assume that the transducer's thermal power intensity distribution shifts in accordance with the shift of the focal spot. Interestingly, one can perceive (2) as the convex combination of the individual profiles, which is much in line with average system dynamics used under fast switching in switched systems.

2.2 State-Space Model

The tissue's temperature profile needs to be controlled in the creation of local hyperthermia and its dynamical behavior is described by a linear Partial Differential Equation (PDE). Before discussing our MPC solution for this challenging control problem, a discretized (in space and time) system formulation is introduced that is amenable for analysis and control design.

As a parabolic PDE, the bio-heat equation (1) can be transformed into an infinite-dimensional system in the frequency domain, Dubljevic et al. (2006). Using the truncated basis functions $U(x) = [u_1(x)\ u_2(x)\ \cdots\ u_n(x)]^T$ and coefficients $\Gamma(t) = [\gamma_1(t)\ \gamma_2(t)\ \cdots\ \gamma_n(t)]^T \in \mathbb{R}^n$, the temperature increment $T(x,t)$ is approximated with

$$T(x,t) = U^T(x)\Gamma(t) = \sum_{i=1}^{n} u_i(x)\gamma_i(t), \tag{3}$$

where the orthogonal basis function $u_i : \mathcal{Q} \to \mathbb{R}$ for $i = 1, 2, \ldots, n$ is defined as $u_i(x) = \sqrt{2/L}\sin(i\pi x/L)$ for $x \in \mathcal{Q}$, such that the boundary conditions in (1) are automatically satisfied. A sufficiently high number n is required to capture the dominant thermodynamics behavior. Adopting the usual $\mathcal{L}_2$ inner product between two functions $u, v : \mathcal{Q} \to \mathbb{R}$ given by $\langle u, v \rangle = \int_{\mathcal{Q}} uv \, \mathrm{d}x$, the Fourier coefficient $\gamma_i(t)$, $i = 1, 2, \ldots, n$, for the temperature distribution $T(\cdot, t)$ can be computed as $\gamma_i(t) = \langle T(\cdot, t), u_i \rangle$. Hence, an Ordinary Differential Equation (ODE) can be derived by substituting (2), (3) into (1) and applying the inner product with u_i. This yields

$$\frac{\mathrm{d}\gamma_i(t)}{\mathrm{d}t} = -\frac{Ki^2\pi^2}{\rho C L^2}\gamma_i(t) - \frac{W_b C_b}{\rho C}\gamma_i(t) + \sum_{j=1}^{m} \frac{p_j(t)}{\rho C}\langle I_j, u_i \rangle. \tag{4}$$

Defining the state-space matrices

$$A = -\frac{K\pi^2}{\rho C L^2}\begin{pmatrix} 1^2 & & 0 \\ & 2^2 & \\ & & \ddots \\ 0 & & n^2 \end{pmatrix} - \frac{W_b C_b}{\rho C} I_n,$$

$$B = \frac{1}{\rho C}\begin{pmatrix} \langle I_1, u_1 \rangle & \langle I_2, u_1 \rangle & \cdots & \langle I_m, u_1 \rangle \\ \langle I_1, u_2 \rangle & \langle I_2, u_2 \rangle & \cdots & \langle I_m, u_2 \rangle \\ \vdots & \vdots & & \vdots \\ \langle I_1, u_n \rangle & \langle I_2, u_n \rangle & \cdots & \langle I_m, u_n \rangle \end{pmatrix}, \tag{5}$$

we obtain the continuous-time linear state-space model of order n given by

$$\begin{aligned}\frac{\mathrm{d}\Gamma(t)}{\mathrm{d}t} =& A\Gamma(t) + BP(t),\\ T(x,t) =& U^T(x)\Gamma(t),\end{aligned} \tag{6}$$

where $P(t) = [p_1(t)\ p_2(t)\ \cdots\ p_m(t)]^T$ is the applied thermal power at every possible focal spot $f_1, f_2, \ldots, f_m$, and $\Gamma(t) = [\gamma_1(t)\ \gamma_2(t)\ \cdots\ \gamma_n(t)]^T$ being the Fourier coefficients representing the temperature distribution $T(\cdot, t)$ at time $t \in \mathbb{R}_{\geqslant 0}$.

The continuous-time state-space model (6) is now discretized in space and time for the ease of implementation of the control strategy. Since the temperature distribution $T(x,t)$ is smooth, it can be represented by the temperature at a well distributed set of sample points $\hat{x}_1, \hat{x}_2, \ldots, \hat{x}_c \in \mathcal{Q}$. A projection matrix that connects state vectors and discretized temperature profiles is defined

$$U_d \triangleq \begin{pmatrix} u_1(\hat{x}_1) & u_1(\hat{x}_2) & \ldots & u_1(\hat{x}_c)\\ u_2(\hat{x}_1) & u_2(\hat{x}_2) & \ldots & u_2(\hat{x}_c)\\ \vdots & \vdots & & \vdots\\ u_n(\hat{x}_1) & u_n(\hat{x}_2) & \ldots & u_n(\hat{x}_c)\end{pmatrix}. \tag{7}$$

With sampling period T_s and the temperature at the sample points as outputs, a discrete-time linear state-space model is obtained with

$$\begin{aligned}\Gamma_{k+1} &= A_d\Gamma_k + B_dP_k,\\ T_k &= U_d^T\Gamma_k,\end{aligned} \tag{8}$$

where $k \in \mathbb{N}$, $T_k = [T(\hat{x}_1, kT_s), T(\hat{x}_2, kT_s), \ldots, T(\hat{x}_c, kT_s)]^T$, $\Gamma_k = \Gamma(kT_s)$, $P_k = P(kT_s)$, $A_d = e^{AT_s}$ and $B_d = \int_0^{T_s} e^{A(T_s-t)}B\mathrm{d}t$. As we will see, this model will be important in the setup of the set-based MPC scheme later.

2.3 Objectives and Problem Formulation

In the creation of local hyperthermia, we have both temperature (output) and power (input) constraints. In order to capture the constraint that the maximum temperature in $\mathcal{Q}$ is restricted below T_{max}, the set of state constraints is given by $\Gamma_k \in \Gamma_{\max} \triangleq \{\Gamma \in \mathbb{R}^n | \mathbf{0}_{c\times 1} \leqslant U_d^T\Gamma \leqslant (T_{max} - T_b)\mathbf{1}_{c\times 1}\}$, $k \in \mathbb{N}$. Note that the inequalities have to be interpreted component-wise. In (2) we have to account for the maximum allowable power input P_{max} for the HIFU transducer, such that $\sum_{i=1}^m p_i(t) \leqslant P_{max}$ for all $t \in \mathbb{R}_{\geqslant 0}$. Considering that the power input can not be negative, the input constraints can be formulated as $P_k \in \mathcal{P} \triangleq \{P \in \mathbb{R}^m \mid \mathbf{1}_{1\times m}P \leqslant P_{max}$ and $P \geqslant \mathbf{0}_{m\times 1}\}$.

To guarantee sufficient therapeutic efficacy, temperature within the treatment region $\mathcal{R}$ needs to be increased to the objective temperature T_{obj}. Meanwhile, the maximum temperature in $\mathcal{Q}$ needs to be kept below the cell killing temperature T_{max} to minimize side effects ($\Gamma_k \in \Gamma_{\max}$). In addition, to avoid unnecessary therapy for surrounding healthy tissue, a steep temperature gradient descent is preferable at the boundary of the treatment region, such that the temperature elevation in $\mathcal{Q} \setminus \mathcal{R}$ is low. Hence, location-dependent lower (T_1) and upper (T_2) bounds of desired temperature profiles can be formulated to ensure a successful creation of local hyperthermia, as illustrated in Fig. 1. Based on these temperature bounds specified at sample points $\hat{x}_1, \hat{x}_2, \ldots, \hat{x}_c$ by values $T_1(\hat{x}_i)$ and $T_2(\hat{x}_i)$, for $i = 1, 2, \ldots, c$, which are stacked in column vectors $T_1 \in \mathbb{R}^c$ and $T_2 \in \mathbb{R}^c$, we can write the set of desirable temperature profiles captured through Γ as

$$\Gamma_{\mathrm{obj}} = \{\Gamma \in \Gamma_{\max} | T_1 \leqslant U_d^T\Gamma + T_b \leqslant T_2\}, \tag{9}$$

where the inequalities are again interpreted component-wise. It is clear that Γ_{obj}, $\Gamma_{\max}$ and $\mathcal{P}$ are high dimensional convex polyhedrons. Although defined in a one-dimensional setup, these concepts extend to a three-dimensional case in a straight forward manner.

Considering that the HIFU transducer can only generate heat with a smooth power intensity profile, the *equilibrium* temperature elevation $T_e(x)$ (such that $K\mathrm{d}^2T_e(x)/\mathrm{d}x - W_bC_bT_e(x) + W_e(x) = 0$) does not have a high temperature gradient at any position. With either insufficient temperature increment in $\mathcal{R}$ or exceeding temperature rise in $\mathcal{Q}\setminus\mathcal{R}$, it does not belong to the objective set and considered undesirable for local hyperthermia. Consequently, there is no equilibria and, in fact, not even a (non-empty) positively (controlled) invariant set in the objective set Γ_{obj}, which contains desired temperature profiles. Although there is no subset within the objective set that can be stabilized, it is possible to shape and maintain *transient* temperature profiles that belong to Γ_{obj} for the therapy duration D_t since body tissue's thermal dynamics is not considered fast. The creation of local hyperthermia can be naturally divided into two phases, which are the heating phase and the therapy (treatment) phase with the duration of D_h and D_t time units, respectively. D_h is expected to be reasonably short to reduce the total therapy duration while D_t is required to be sufficiently long to ensure therapeutic efficacy. With fixed sampling period T_s, $N_h \in \mathbb{N}$ and $N_t \in \mathbb{N}$ denote the time steps taken in the heating and therapy phases, respectively, we assume $(N_h - 1)T_s < D_h \leqslant N_hT_s$ and $(N_t - 1)T_s < D_t \leqslant N_tT_s$. Therefore, the control objective for local hyperthermia can be formalized as to find a control strategy that for each $k = 0, 1, \ldots, N_h + N_t$, determines the control input $P_k \in \mathcal{P}$, based on the state vector Γ_k, such that for all $k = 0, 1, \ldots, N_h + N_t$ it holds that $\Gamma_k \in \Gamma_{\max}$, and for all $k = N_h, N_h + 1, \ldots, N_h + N_t$ it holds that $\Gamma_k \in \Gamma_{\mathrm{obj}}$ (if possible, given D_h and D_t).

3. CONTROLLER DESIGN

As already mentioned, with either insufficient temperature increment in $\mathcal{R}$ or exceeding temperature rise in $\mathcal{Q} \setminus \mathcal{R}$, there is no equilibrium nor a (controlled) positively invariant set of temperature distribution in the desired set of temperature profiles. Hence, it is not possible to stay in the objective set for infinitely long time. Due to this non-standard setting, a novel MPC method is needed, which we introduce in this section.

3.1 Set Reachability Analysis

Based on the control objectives discussed in the previous section, it is important to verify the feasibility of the control goals (given the desired heating and therapy durations D_h and D_t, respectively). For that reason, it is important to carry out a set-based analysis to find the set of (initial) states Γ for which it is possible to remain N_t steps inside Γ_{obj}, while satisfying the input constraints. This set will be denoted by Γ_{ref} and should be non-empty to be able to fulfill the control objectives just formalized. If Γ_{ref} is empty, D_t and/or Γ_{obj} should be adjusted. Assuming that Γ_{ref} is not empty, then this is the set we should reach at discrete time step N_h. Hence, to verify the feasibility of the first phase in the control objective (reaching this set), a reachability analysis needs to be carried out to see if we can actually reach this set from $\Gamma_0 \triangleq \mathbf{0}_{n\times 1}$ in N_h steps. If not, N_h or the set Γ_{ref} should be modified. Therefore, we define the N-step backwards reachability set from $\mathcal{F}$ with the state and power constraints set $\mathcal{G}$ and $\mathcal{P}$, respectively

$$\begin{aligned}\mathbf{\Gamma}^{(N)}(\mathcal{F},\mathcal{G},\mathcal{P}) =& \{\Gamma \in \mathbb{R}^n | \exists \mathbf{P} = [P_0, \ldots, P_{N-1}], \text{s.t. } P_k \in \mathcal{P},\\ & \mathcal{X}_N(\Gamma, \mathbf{P}) \in \mathcal{F} \text{ and } \mathcal{X}_k(\Gamma, \mathbf{P}) \in \mathcal{G} \text{ for } k = 0, 1, \ldots, N\},\end{aligned} \tag{10}$$

where $\mathcal{X}_k(\Gamma, \mathbf{P})$ denotes the solution to (8) at time $k = 0, 1, 2, \ldots, N$ starting with initial state $\Gamma_0 = \Gamma$ and with input sequence $\mathbf{P}$. As the control objective is to keep the state vector Γ_k in Γ_{obj} for N_t steps, the reference set $\Gamma_{\text{ref}} = \mathbf{\Gamma}^{(N_t)}(\Gamma_{\text{obj}}, \Gamma_{\text{obj}}, \mathcal{P})$ needs to be computed to show the feasibility of the control objective.

Based on the method suggested in (Blanchini and Miani, 2008, p. 157), a schematic procedure to compute the set (10) given sets $\mathcal{F}$, $\mathcal{G}$ and $\mathcal{P}$ is

(1) Set $k = 0$ and $\Gamma^{(k)} = \mathcal{F} \cap \mathcal{G}$.
(2) If $\Gamma^{(k)} = \emptyset$ or $k = N_t$, then stop.
(3) Compute set $\Gamma^{(k+1)} = \{\Gamma \in \mathcal{G} | \exists P \in \mathcal{P}$ s.t. $A_d\Gamma + B_dP \in \Gamma^{(k)}\}$.
(4) Set $k = k + 1$ and go to step 2.

This computation is iterative and does not need to be solved on-line. Hence, to verify the feasibility of our control objectives, we perform the following tasks:

(1) Compute $\Gamma_{\text{ref}} = \mathbf{\Gamma}^{(N_t)}(\Gamma_{\text{obj}}, \Gamma_{\text{obj}}, \mathcal{P})$ and assume it is non-empty (otherwise adapt Γ_{obj} or N_t).
(2) Compute $\mathbf{\Gamma}^{(N_h)}(\Gamma_{\text{ref}}, \Gamma_{\max}, \mathcal{P})$ and check if the initial state $\Gamma_0 \in \mathbf{\Gamma}^{(N_h)}(\Gamma_{\text{ref}}, \Gamma_{\max}, \mathcal{P})$, (if not, adjust N_h or Γ_{ref} through step 1).

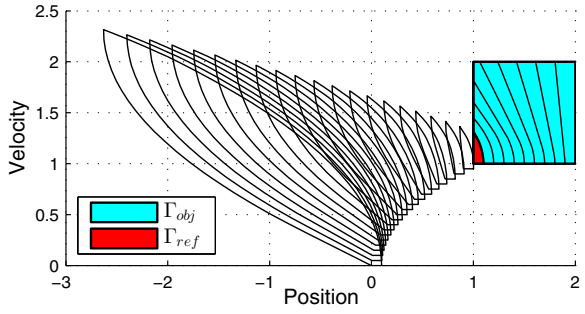

Fig. 2. Reachability analysis illustrated with a double integrator system

To illustrate the reachability analysis through this procedure, we consider the discrete-time double integrator

$$x_{k+1} = \begin{pmatrix} 1 & T_s \\ 0 & 1 \end{pmatrix} x_k + \begin{pmatrix} 0.5T_s^2 \\ T_s \end{pmatrix} u_k, \tag{11}$$

where $x_k \in \mathbb{R}^2$, $u_k \in \mathbb{R}$, $k \in \mathbb{N}$ and the sampling period $T_s = 0.1$. The objective set is defined as $\Gamma_{\text{obj}} = \{x \in \mathbb{R}^2 | 1 \leqslant x_1 \leqslant 2, 1 \leqslant x_2 \leqslant 2\}$ and $N_t = 9$. Containing only positive velocity, the objective set Γ_{obj} does not include an equilibrium or a (non-empty) controlled positively invariant set. By following the reachability analysis method just introduced, a reference set $\Gamma_{\text{ref}} = \mathbf{\Gamma}^{(9)}(\Gamma_{\text{obj}}, \Gamma_{\text{obj}}, \mathbb{R})$ is computed and plotted in Fig. 2. The reference set is, as expected, located in the lower-left corner of the objective set. The feasibility check can be executed by computing the backwards reachability sets originating from Γ_{ref} until the initial state $x_0 = [0, 0]^T$ is included. In this case, the feasibility is confirmed with $N_h = 20$. All backwards reachability sets are plotted with black lines in Fig. 2.

3.2 Dual-Mode MPC

Assuming that the reachability set tests are passed successfully, a dual-mode MPC is proposed to fulfill all objectives. It consists of two MPC schemes $\mathcal{C}_h$ and $\mathcal{C}_t$ in the heating and therapy phase, respectively. In mode one (heating phase), the controller $\mathcal{C}_h$ regulates the state vector to Γ_{ref} at time step N_h. The controller $\mathcal{C}_h$ at time step $k \in \mathbb{N}$ with state vector Γ_k in the heating phase is

$$\begin{aligned} \min_{\substack{\mathbf{P_k} \triangleq [P_{k|k}, P_{k+1|k}, \ \ldots \ , P_{N_h|k}] \\ \epsilon_{\mathbf{k}} \triangleq [\epsilon_{k|k}, \ \epsilon_{k+1|k}, \ldots, \epsilon_{N_h|k}]}} & \left\{ J(\Gamma_k, \mathbf{P_k}) = \sum_{i=k}^{N_h} \epsilon_{i|k}^2 \right\}, \\ s.t. \ & \Gamma_{N_h|k} \in \Gamma_{\text{ref}}, \ P_{i|k} \in \mathcal{P}, \ i = k, k+1, \ldots, N_h, \\ & U_d^T \Gamma_{i|k} + T_b \geqslant T_1 - \epsilon_{i|k} \mathbf{1}_{n \times 1}, \ i = k, k+1, \ldots, N_h, \\ & U_d^T \Gamma_{i|k} + T_b \leqslant T_2, \ i = k, k+1, \ldots, N_h, \\ & \Gamma_{i+1|k} = A_d \Gamma_{i|k} + B_d P_{i|k}, \ \Gamma_{k|k} = \Gamma_k, \end{aligned} \tag{12}$$

with a minimizer $\mathbf{P_k^*} = \left[P_{k|k}^*, P_{k+1|k}^*, \ \ldots \ , P_{N_h|k}^*\right]$ and $\epsilon_{\mathbf{k}}^* = \left[\epsilon_k^*, \ \epsilon_{k+1|k}^*, \ldots, \epsilon_{N_h|k}^*\right]$. The control law for $k = 0, 1, \ldots, N_h - 1$ is then given by $P_k = P_{k|k}^*$. Note that this MPC formulation uses slack variables $\epsilon_{i|k} \in \mathbb{R}$ to capture the difference between the predicted temperature profiles and the desired set of temperature distributions, similar to the formulation of soft constraints as used in, e.g., Kerrigan and Maciejowski (2000).

In mode two (therapy phase), Γ_k has to be kept inside Γ_{obj} by the controller $\mathcal{C}_t$ for N_t steps. The controller $\mathcal{C}_t$ at time step $k = N_h, N_{h+1}, \ldots, N_h + N_t - 1$ with state vector Γ_k in the therapy phase is given by

$$\begin{aligned} \min_{\mathbf{P_k} \triangleq [P_{k|k}, \ \ldots \ , P_{N_h+N_t-1|k}]} & \left\{ J(\Gamma_k, \mathbf{P_k}) = \sum_{i=k}^{N_h+N_t-1} \sum_{j=1}^{m} p_j \right\}, \\ s.t. \ & P_{i|k} \in \mathcal{P}, \ \Gamma_{i|k} \in \Gamma_{\text{obj}}, \ i = k, \ldots, N_h + N_t, \\ & \Gamma_{i+1|k} = A_d \Gamma_{i|k} + B_d P_{i|k}, \ \Gamma_{k|k} = \Gamma_k, \end{aligned} \tag{13}$$

with a minimizer $\mathbf{P_k^*} = \left[P_{k|k}^*, \ \ldots \ , P_{N_h+N_t-1|k}^*\right]$. The control law for $k = N_h, N_h + 1, \ldots, N_h + N_t - 1$ is then given by $P_k = P_{k|k}^*$. Note that both (12) and (13) have a shrinking horizon. Based on the above developments, we can now establish the following theorem.

Theorem 1. Assume N_h, N_t, $\mathcal{P}$ and Γ_{obj} are such that

- $\Gamma_{\text{ref}} = \mathbf{\Gamma}^{(N_t)}(\Gamma_{\text{obj}}, \Gamma_{\text{obj}}, \mathcal{P}) \neq \emptyset$
- $\Gamma_0 \in \mathbf{\Gamma}^{(N_h)}(\Gamma_{\text{ref}}, \Gamma_{\max}, \mathcal{P})$

Consider system (8) in closed loop with the dual-mode controller given by $P_k = P_{k|k}^*$ with $\mathbf{P_k^*}$, which is obtained from problem (12) for $k = 0, 1, \ldots, N_h - 1$ and from (13) for $k = N_h, N_h + 1, \ldots N_h + N_t - 1$. This closed-loop system satisfies for initial condition Γ_0 that

- $\Gamma_k \in \Gamma_{\max}$ and $P_k \in \mathcal{P}$, for $k = 0, 1, 2, \ldots, N_h + N_t$;
- $\Gamma_k \in \Gamma_{\text{obj}}$, for $k = N_h, N_h + 1, \ldots, N_h + N_t$.

Hence, the proposed controller solves the problem considered in this paper.

4. NUMERICAL ILLUSTRATION

The performance of our dual-mode MPC scheme will now be verified for the one-dimensional case study discussed in Section 2 using the parameters listed in Table 1. All parameters were chosen so that the simulation is comparable to the practical application and we have $\mathcal{R} \subset \mathcal{Q}$. The computation of the set Γ_{ref} and the reachability analysis were

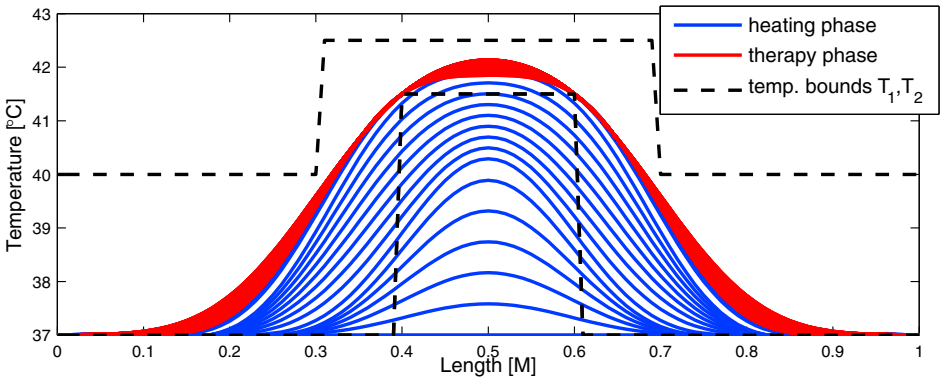

Fig. 3. Temperature evolution with temperature distributions in both the heating phase (blue) and the therapy phase (red) and the objective temperature distribution's lower and upper bounds (T_1, T_2) are plotted in dashed lines.

carried out using the Multi-Parametric Toolbox (MPT), Kvasnica et al. (2004).

Table 1. Specifications on geometry and model parameters in the one-dimensional setting

C	3500	T_{obj}	41.5	D_h	200	T_s	10
ρ	1000	T_{max}	42.5	D_t	1400	m	6
K	5	P_{max}	30	N_h	20	n	10
W_b	0.3	T_b	37	N_t	140	$\mathcal{Q}$	$[0,1]$
F	$\{0.3, 0.38, 0.46, 0.54, 0.62, 0.7\}$			$\mathcal{R}$	$[0.4, 0.6]$		

Since the reachability set computation (with a polyhedron type input constraint set) in a high-dimensional state space is quite demanding even when using MPT, the feasibility check that we introduced in Section 3.1 was not carried out in the presented form. Instead of Γ_{ref}, we computed Γ'_{ref} given by

$$\Gamma'_{\text{ref}} = \{\Gamma \in \mathbb{R}^n | \mathcal{X}_k(\Gamma, \mathbf{P}') \in \Gamma_{\text{obj}},\ k = 1, 2, \ldots, N'_t\},$$
$$s.t.\ \mathbf{P}' = [P', P', \ldots, P'] \text{ with } P' = [0, p', 0, 0, p', 0]^T, \tag{14}$$

where $N_t > N'_t = 10$ and $p' = 2.5$. The computational effort in finding the reference set is greatly reduced by allowing the usage of only one input value being $P' \in \mathcal{P}$, which helps to avoid computing the Minkowski sum of high-dimensional polyhedrons. Since the power input at the boundary of the treatment region is needed in the therapy phase to maintain sufficient temperature increment in $\mathcal{R}$, constant power inputs were assigned at f_2 and f_5 for the computation of Γ'_{ref}. By choosing Γ'_{ref} as the reference set, the computed controller still managed to create a local hyperthermia and met all specifications listed in Table 1, which is demonstrated by the simulation results.

The simulation results containing the evolution of the temperature profiles in the heating phase (blue) and in the therapy phase (red) as well as the objective temperature distribution's lower and upper bounds T_1 and T_2 (dashed) are plotted in Fig. 3. In the heating phase, the temperature in $\mathcal{R}$ was increased up to T_{obj} and the temperature distribution was kept in the desired temperature profile set in the therapy phase. Although no direct thermal power was applied outside the treatment region, significant temperature elevation in $\mathcal{Q} \setminus \mathcal{R}$ can be observed in the therapy phase due to heat conduction. In both phases, the maximum temperature constraint T_{max} was not violated and the temperature increment outside the treatment region remained below the upper bound T_2. For detailed information about the temperature profile evolution trajectory and corresponding thermal intensity profile in both the heating and the therapy phase, multiple

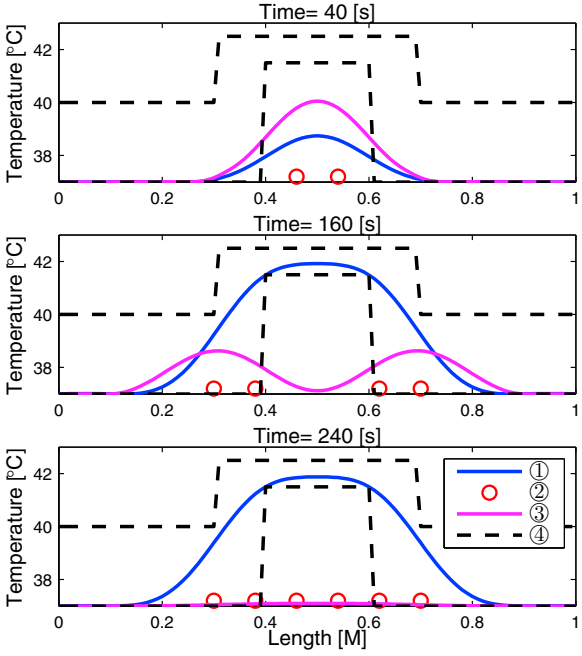

Fig. 4. Evolution snapshots. ① temperature distribution, ② active focal spots, ③ total thermal power intensity distribution, ④ temperature lower and upper bounds.

snapshots are plotted in Fig. 4. It contains temperature profiles, active focal spots, total thermal power intensity and temperature lower and upper bounds at different time instants. It can be observed that a large amount of thermal energy was applied in the center of treatment region in the beginning while focal spots close to the boundary were activated in the end of heating phase. Such an efficient way of building up temperature elevation in a treatment region is expected with the application of $\mathcal{C}_h$ as it computed the optimal evolution trajectory for temperature profiles and corresponding focal spots were activated with optimal power level. During the therapy phase, all focal spots were activated with low power input to maintain sufficient temperature increment in $\mathcal{R}$. To check the quality of created local hyperthermia, the difference between the temperature profile $T(x)$ is compared to the set of desired temperature profiles at the sample points $\hat{x}_1, \hat{x}_2, \ldots, \hat{x}_c$

$$\varepsilon = \max(0, T_1(\hat{x}_1) - T(\hat{x}_1) - T_b, \ldots, T_1(\hat{x}_c) - T(\hat{x}_c) - T_b). \tag{15}$$

In both the heating and the therapy phase, the total power input and the distance measurement ε are plotted in Fig.

5. In the heating phase, the maximum power level was reached to heat tissue as quickly as possible and ε decreased fast. A significant power drop occurred at the end of the heating phase ($k = N_h$). Then, the total power input stayed constant and the changing temperature profile was maintained inside the objective set ($\varepsilon = 0$). This reveals a small temperature variance within the treatment region during the therapy phase as the boundaries of the set of desired temperature profiles are tight.

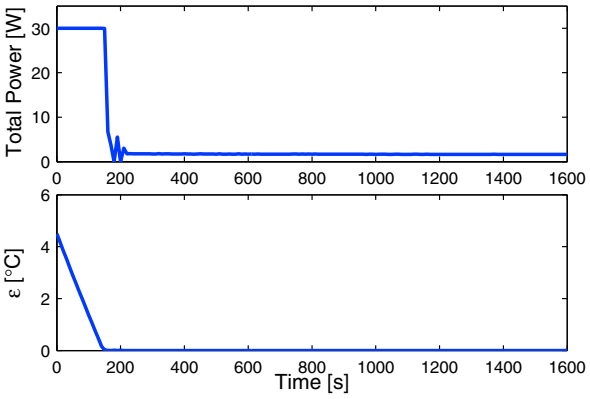

Fig. 5. Total input power and the difference between the measured temperature distribution and the set of desired profiles expressed through the distance measurement ε.

It is clear that the proposed dual-mode MPC scheme $\mathcal{C}_h$ (12) and $\mathcal{C}_t$ (13) successfully controlled the temperature distribution in $\mathcal{Q}$ and a satisfactory local hyperthermia was achieved fulfilling all control objectives, including temperature profile requirements and state and input constraints. With smaller temperature variance inside the treatment region, our novel dual-mode MPC scheme leads to an enhanced local hyperthermia for cancer treatment compared to currently available controllers such as the ones in Mougenot et al. (2009); Salomir et al. (2000).

5. CONCLUSIONS

In this paper, a novel MPC approach is presented for creating local hyperthermia to enhance cancer treatment. It overcomes the limitations that existing control strategies for this problem have. This new MPC scheme has a few interesting novelties. First of all, the MPC scheme regulates the state towards a desired set instead of a single point, which is different from many existing approaches and even different from robust MPC approaches that also drive the state to the set, but this is mainly due to the presence of disturbances. Secondly, the set we aim to reach does not contain any equilibrium state nor a positively (controlled) invariant subset. These features leads us to define a new (dual-mode) setup based on set-based (reachability) analysis. Using this analysis immediately gives the feasibility guarantee of the proposed scheme. A one dimensional simulation showed that the desired temperature distribution is kept inside the objective set during the therapy phase without violating both maximum temperature and maximum power constraints, which shows the strengths of the proposed scheme. An issue for future work is to consider the reachability set computation given the high order dimensions. It is of interest to investigate better algorithms for its computations, potentially using reduced order models or improved MPC schemes (e.g. with shorter horizons, but time-varying target sets). The relevance of the applications domain will spur further developments in these directions in the future.

REFERENCES

Blanchini, F. and Miani, S. (2008). *Set-Theoretic Methods in Control*. Birkhäuser.

Camacho, E. and Bordons, C. (2007). *Model Predictive Control*. Springer.

de Smet, M., Heijman, E., Langereis, S., Hijnen, N.M., and Grüll, H. (2011). Magnetic resonance imaging of high intensity focused ultrasound mediated drug delivery from temperature-sensitive liposomes: An *in vivo* proof-of-concept study. *Journal of Controlled Release*, 150(1), 102–110.

Dubljevic, S., El-Farra, N.H., Prashant, M., and Christofides, P.D. (2006). Predictive control of parabolic PDEs with state and control constraints. *Internat. J. Robust Nonlinear Control*, 16(16), 749–772.

Gaber, M., Hong, K., Huang, S., and Papahadjopoulos, D. (1995). Thermosensitive sterically stabilized liposomes: Formulation and in vitro studies on mechanism of doxorubicin release by bovine serum and human plasma. *Pharmaceutical Research*, 12(10), 1407–1416.

Hijnen, N.M., Heijman, E., Köhler, M.O., Ylihautala, M., Ehnholm, G.J., Simonetti, A.W., and Grüll, H. (2012). Tumour hyperthermia and ablation in rats using a clinical MR-HIFU system equipped with a dedicated small animal set-up. *Int. J. Hyperthermia*, 28(2), 141–155.

Hynynen, K., Clement, G., McDannold, N., Vykhodtseva, N., King, R., White, P., Vitek, S., and Jolesz, F. (2004). 500-element ultrasound phased array system for noninvasive focal surgery of the brain: A preliminary rabbit study with ex vivo human skulls. *Magnetic Resonance in Medicine*, 52(1), 100–107.

Issels, R.D. (2008). Hyperthermia adds to chemotherapy. *European Journal of Cancer*, 44(17), 2546–2554.

Kerrigan, E. and Maciejowski, J. (2000). Soft constraints and exact penalty functions in model predictive control. *Control 2000 Conference, Cambridge*.

Kvasnica, M., Grieder, P., and Baoti, M. (2004). Multi-parametric toolbox (MPT).

Maciejowski, J. (2002). *Predictive Control with Constraints*. Prentice Hall.

Mayne, D.Q., Rawlings, J.B., Rao, C.V., and Scokaert, P.O.M. (2000). Constrained model predictive control: Stability and optimality. *Automatica*, 36(2000), 789–814.

Mougenot, C., Quesson, B., de Senneville, B., de Oliveira, P., Sprinkhuizen, S., Palussière, J., Grenier, N., and Moonen, C. (2009). Three-dimensional spatial and temporal temperature control with MR thermometry-guided focused ultrasound (MRgHIFU). *Magnetic Resonance in Medicine*, 61(3), 603–614.

Overgaard, J. (1989). The current and potential role of hyperthermia in radiotherapy. *International Journal of Radiation Oncology*Biology*Physics*, 16(3), 535–549.

Rawlings, J. and Mayne, D. (2013). *Model Predictive Control: Theory and Design*. Nob Hill Publishing.

Rieke, V. and Pauly, K.B. (2008). MR thermometry. *J. Magn. Reson. Imaging*, 27(2), 376–390.

Salomir, R., J.Palussière, Vimeux, F., de Zwart, J., Quesson, B., Gauchet, M., Lelong, P., Pergrale, J., Grenier, N., and Moonen, C. (2000). Local hyperthermia with MR-guided focused ultrasound: spiral trajectory of the focal point optimized for temperature uniformity in the target region. *J. Magn. Reson. Imaging*, 12(4), 571–583.

Wissler, E. (1998). Pennes' 1948 paper revisited. *J. Appl. Physiol.*, 85(1), 35–41.